Polymer 49 (2008) 4602–4611

Contents lists available at ScienceDirect

Polymer

journal homepage: www.elsevier.com/locate/polymer

Preparation and properties of biodegradable PBS/multi-walled carbon nanotube nanocomposites

Y.F. Shih [a,*], L.S. Chen [b], R.J. Jeng [b]

[a] Department of Applied Chemistry, Chaoyang University of Technology, 168 Jifong East Road, Wufong Township, Taichung County 41349, Taiwan
[b] Department of Chemical Engineering, National Chung Hsing University, 250 Kuo Kuang Road, Taichung 402, Taiwan

ARTICLE INFO

Article history:
Received 25 May 2008
Received in revised form 6 August 2008
Accepted 8 August 2008
Available online 14 August 2008

Keywords:
Multi-walled carbon nanotubes
Biodegradable
Poly(butylene succinate)

ABSTRACT

In this study, poly(butylene succinate)/multi-walled carbon nanotube (PBS/MWNT) hybrids were prepared by a melt-blending process. The carbon nanotubes (CNTs) were successfully modified using *N*,*N*′-dicyclohexylcarbodiimide (DCC) dehydrating agents. As a result, excellent dispersion of the modified carbon nanotubes (CNT–C18) in organic solvents was achieved. Subsequently, the PBS/CNT nanocomposites were prepared through facile melt blending. Mechanical properties, thermal behavior, conductivity of these resultant polymer/CNT composites were investigated. The results obtained show that the PBS/CNT–C18 nanocomposites consisting of well-dispersed nanotubes exhibited enhanced thermal and mechanical properties. With the addition of 3 wt% CNT–C18, T_d of the nanocomposite increased 12.3 °C as compared to that of the pristine PBS sample. Moreover, the increments of E' and E'' of the nanocomposite at 25 °C were 120 and 55%, respectively. In the aspect of conductivity, the surface resistivity of the PBS/CNT–C18 composite was found to be 7.30×10^6 Ω, which is a decrease of 10^9 fold in value as compared to that of the pristine PBS sample. Such PBS/CNT–C18 sample exhibits high anti-static efficiency, which would be potentially useful in electronic packaging materials.

1. Introduction

Recently, the development of biodegradable polymers has attracted a great deal of interest, because environmental pollution problems are getting more serious. Aliphatic polyesters are among the most promising materials to be considered as high performance environmentally friendly biodegradable plastics [1–3]. One of these aliphatic polyesters is poly(butylene succinate) (PBS), known under the trade name "Bionolle". Bionolle is synthesized through the polycondensation reaction of glycols such as ethylene glycol and 1,4-butanediol, and aliphatic dicarboxylic acids such as succinic acid and adipic acid. This white crystalline thermoplastic polymer exhibits not only a melting point similar to that of low-density polyethylene (LDPE), but also glass transition temperature (T_g) and tensile strength between those of polyethylene (PE) and poly(propylene) (PP), and stiffness between that of LDPE and high-density polyethylene (HDPE). In addition, this biodegradable polymer possesses satisfactory strength and toughness, close to those of LDPE [4], which is considered highly promising as a commercial commodity polymer.

Since the first observation of carbon nanotubes (CNTs) in 1991 by Iijima [5], and the awareness of their distinctive mechanical, thermal and electrical properties, extensive researches in the field of CNT/polymer nanocomposites have been pursued. CNTs often aggregate to bundles due to the van der Waals interactions between individual tubes, which constitutes a major limitation in polymer composite applications [6,7]. Recently, many studies are focused on the preparation of polymer/CNT composites via melt mixing. This is because high temperature and large shear forces in melt mixing often cause chemical and/or physical interactions between inorganic fillers and polymer components. These understandings have been confirmed by both theoretical and experimental studies [8,9]. Moreover, via solution mixing, the utilization of excessive toxic and/or volatile solvents makes these methods impractical for bulk production of polymer/CNT composites.

According to literature [10], the optimal amount of multi-walled carbon nanotubes (MWNTs) is only 1 wt% because excessive MWNT would cause separation of the organic and inorganic phases and lowered their compatibility. CNTs are generally insoluble in organic solvents. Therefore, the organic modification of CNTs to increase their organophilic properties is required for many industrial applications. One approach is to take advantage of the oxidative formation of carboxyl functionalities, and to graft organic moieties onto the tubes subsequently. A great deal of research efforts followed this route to the preparation of soluble nanotubes [11,12]. Chen et al. [13] first used long-chain molecule to modify single-walled carbon nanotubes (SWNTs) via formation of the amide functionality to increase the solubility of the SWNTs in

* Corresponding author. Tel.: +886 4 23323000x4586; fax: +886 4 23742341.
E-mail address: syf@cyut.edu.tw (Y.F. Shih).

0032-3861/$ – see front matter © 2008 Elsevier Ltd. All rights reserved.
doi:10.1016/j.polymer.2008.08.015

organic solvents. Firstly, the SWNTs were treated by $SOCl_2$. Subsequently, the treated SWNTs were reacted with octadecylamine (ODA) to form the modified SWNTs, which were soluble in chloroform, dichloromethane, aromatic solvents (benzene, toluene, chlorobenzene, 1,2-dichlorobenzene), and CS_2. More recently, Chen and Zhang [14] mixed the acidified SWNTs with ODA and *N*,*N*′-dicyclohexylcarbodiimide (DCC) to graft the ODA onto SWNTs. The solubility and dispersion of SWNTs were greatly enhanced by this surface modification treatment. In contrast to the pristine SWNTs which are insoluble in organic solvents, the modified SWNTs manifest a substantial solubility and good dispersion in many kinds of organic solvents such as chloroform, dichloromethane, carbon disulfide, etc. In addition, the surface modification might contribute to the weakening of the mutual attractive forces between SWNTs, causing exfoliation of the SWNT bundles to give well-dispersed individual nanotubes. Moreover, Lin et al. [15] demonstrated the feasibility of functionalizing MWNTs with carbonyl derivatives through oxidation. Subsequently, amphiphilic properties were introduced by grafting the poly(oxyalkylene)-amine (POA-amine) pendants via amide linkages. Three different amidation routes for grafting high-molecular weight POA-amines onto MWNTs were investigated: (1) direct thermal amidation, (2) acylation-mediated amidation, (3) DCC-coupling amidation. By comparison, the DCC-coupling method is more effective for grafting diamines onto MWNT–COOH via the amide linkages.

Even though the researches about polymer/CNT composites grow rapidly, the preparation of biodegradable polymer/CNT composites remains rare. Most of the researches were focused on the polylactide/CNT (PLA/CNT) composites [10,16–18]. However, the characteristics and applications of PBS are quite different from those of PLA. PBS is more suitable to replace the usage of PE or PP than PLA. Moreover, most of the biodegradable polymer/CNT composites were prepared directly by mixing the biodegradable polymer with the acidified CNT [16,19], or through in situ polymerization [17,18,20]. In these cases, the CNTs were not modified chemically to improve their dispersion in the polymer matrices. Wu and Liao [10] prepared polylactide/multi-walled carbon nanotube (PLA/MWNT) hybrids by melt blending. To better enhance the compatibility between PLA and MWNTs, the acrylic acid grafted polylactide (PLA-*g*-AA) and the multihydroxyl-functionalized MWNTs (MWNTseOH) were blended to form the PLA/MWNT hybrids. Due to the formation of ester groups through the reaction between carboxylic acid groups of PLA-*g*-AA and hydroxyl groups of MWNTseOH, significant enhancement in thermal and mechanical properties of PLA with the addition of only 1 wt% was achieved. However, it was found that the optimal amount of MWNTseOH was 1 wt% because excessive MWNTseOH would cause separation of the organic and inorganic phases and lower their compatibility. In addition, Ray et al. [21] prepared the PBS/MWNT nanocomposite by melt blending in a batch mixer. Substantial enhancement in the mechanical properties of PBS was also observed. The storage flexural modulus increased from 0.64 GPa for pristine PBS to 1.2 GPa for the nanocomposite with 3 wt% of MWNTs. The electrical conductivity of the nanocomposite dramatically increased as compared to that of the pristine PBS sample. The in-plane conductivity increased from 5.8×10^{-9} S/cm for neat PBS to 4.4×10^{-3} S/cm for nanocomposite, an increase of 10^6 fold in value of the electrical conductivity. In this study, we modified the CNT first by using the DCC-coupling method to introduce the long alkyl chain onto the MWNTs, so as to reduce the aggregation of CNTs, and to improve the compatibility between CNTs and polymers. Subsequently, the PBS/CNT nanocomposites were prepared through melt blending. As a result, the MWNTs would disperse well in the polymer matrices. Moreover, mechanical properties, thermal behavior, conductivity of these resultant polymer/CNT composites can be further enhanced.

2. Experimental

Polybutylene succinate (PBS, Bionolle#1020) was supplied by Showa Highpolymer Co. Ltd., Japan. In order to enhance the compatibility between PBS and multi-walled carbon nanotubes (obtained from the Desunnano Co., Taiwan), the surface modification of CNTs was achieved as the following. Firstly, purified CNTs were dispersed in HNO_3, and kept at 120 °C for 40 min in the reflux system, to introduce the carboxyl groups at their opening ends and defect locations on their walls. The CNT–COOH could be dispersed in dry DMF and mixed stearyl alcohol and *N*,*N*′-dicyclohexylcarbodiimide (DCC) [14,15,22]. Subsequently, the stearyl alcohol was grafted onto CNTs at room temperature for 48 h (Scheme 1). The proposed mechanism of C18 grafting onto CNT via DCC process is shown in Scheme 2(a) and (b) [14,15]. One possible mechanism is DCC catalyzed esterification (Scheme 2(a)), and the other one is DCC dehydration (Scheme 2(b)). This modified CNT–C18 would exhibit good dispersion in organic solvents, because the presence of the long alkyl chain played a critical role in the solubilization process [23].

The PBS/CNT nanocomposites were prepared through melt blending in a counter-rotating internal mixer (Brabender PL2000, Duisburg, Germany) with a rotation speed of 60 rpm for 5 min at 120 °C. Samples for the investigations were prepared by compression molding under 180 kgf/cm^2 at 140 °C for 3 min, and then solidification by quenching in ambient temperature. The illustration of the melt-blending process is shown in Scheme 3.

Thermogravimetric analyses (TGAs) were performed using a TA Q-500 analyzer. Samples were heated from room temperature to 800 °C at a heating rate of 20 °C/min under nitrogen. Crystallization behavior was analyzed by differential scanning calorimeter (DSC; Seiko SII Model SSC5200). Samples were firstly heated from room temperature to 180 °C at a heating rate of 10 °C/min, and then held at 180 °C for 10 min. Subsequently, these samples were cooled from 180 °C to room temperature at a cooling rate of 10 °C/min (1st cooling). Then, the samples were again heated from room temperature to 180 °C at a heating rate of 10 °C/min (2nd heating). Dynamic mechanical behaviors of the

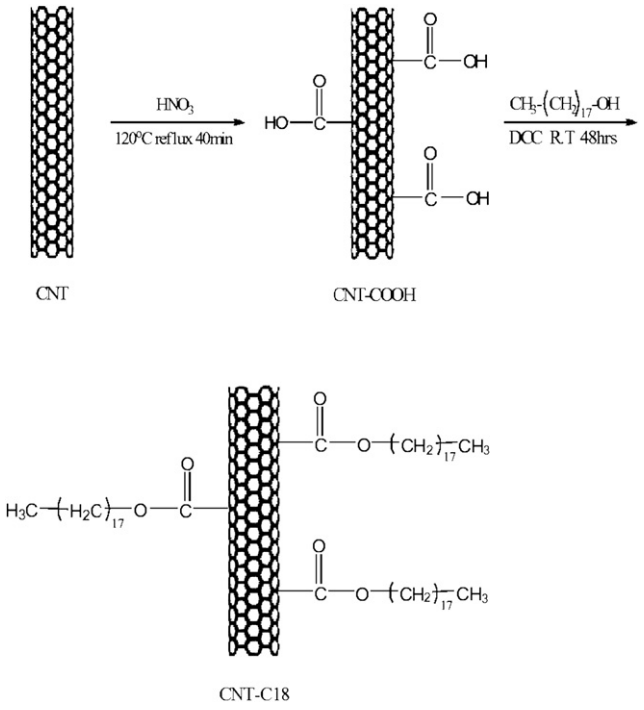

Scheme 1. Surface modification of multi-walled carbon nanotubes.

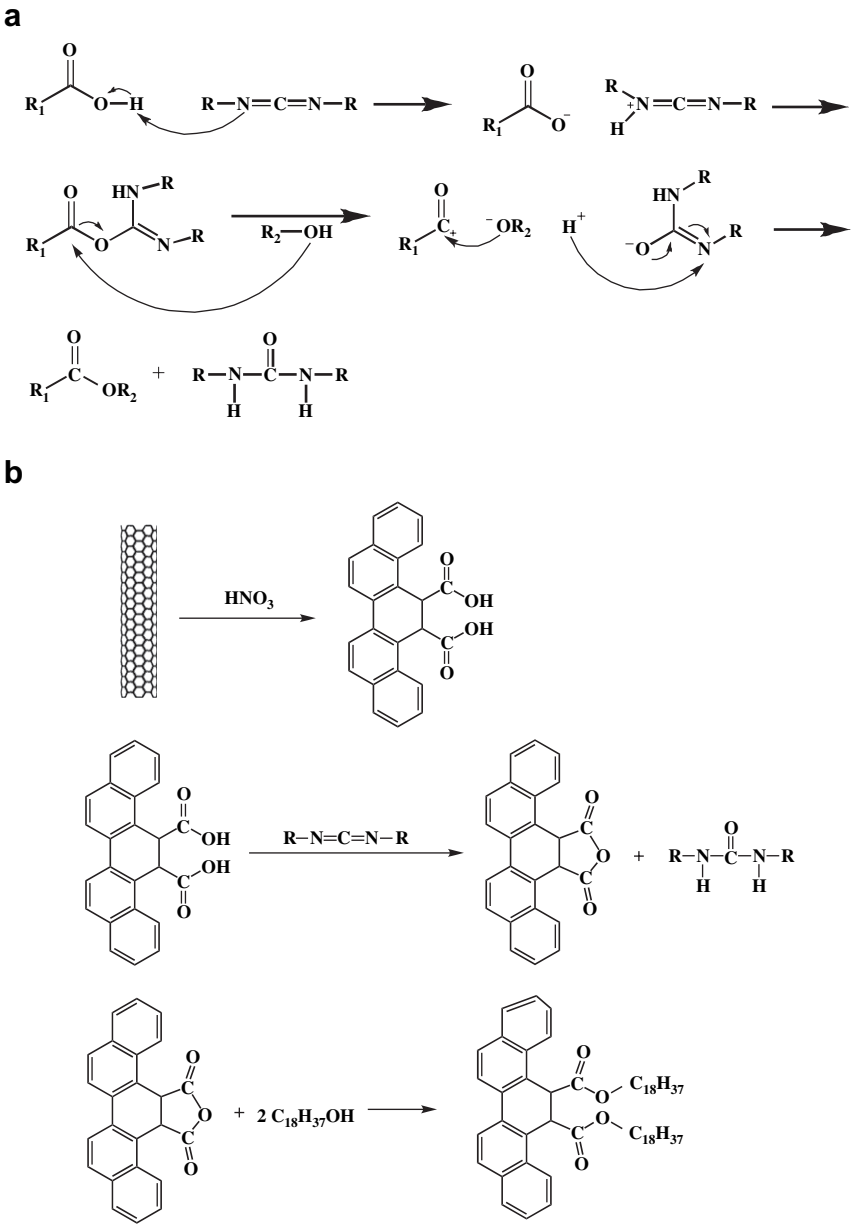

Scheme 2. The proposed mechanism of grafting C18 onto CNT via DCC process.

nanocomposites were measured by PERKIN ELMER DMA 7E. The dimensions of the samples were 1.5 mm × 18 mm × 10 mm, whereas the test was performed in the three-point bending mode at a frequency of 1 Hz. Surface resistivity of the nanocomposites was measured using TOADKK SME-8310 super mega ohm meter, according to the ASTM D257 method. Scanning electron microscope (SEM) (JEOL JSM-6700F) was used to observe the fractured surface of PBS/CNT nanocomposites with different CNT contents. Transmission electron microscopy (TEM) was carried out on JEOL JEM-1200CXII.

3. Results and discussion

3.1. Characterization of the organically grafted CNTs

Fig. 1(a) shows that hydrophilicity and hydrophobicity were absent in the pristine carbon nanotubes (u-CNT). However, the dispersibility of CNT–COOH was remarkably changed after modification. CNT–COOH was hydrophilic and well dispersed in water (Fig. 1(b)), whereas CNT–C18, consisting of long alkyl chains, was hydrophobic and dispersible in chloroform (Fig. 1(c)).

After modification, the thermal stability of carbon nanotubes was decreased due to the organic modification (Fig. 2). The attached organic content was estimated according to the residual weight of the functionalized CNTs at 500 °C [24]. The estimated organic attachment content of CNT-18 is 5.4 wt%. Because of strong intrinsic van der Waals forces, CNTs tend to hold together as ropes and bundles, exhibiting very low solubility in most solvents. The u-CNT sample could be highly entangled with one another and form an interconnecting structure (Fig. 3(a)) [25]. On the other hand, Fig. 3(b) and (c) shows that CNT–COOH and CNT–C18 were well dispersed through acid treatment and chemical modification. Yet the length of nanotubes remained about 600–1000 nm. Via acid treatment, u-CNT was oxidized to form CNT–COOH, which was soluble in water. Moreover, the length of CNT–COOH became somewhat shorter, indicating that the entangled phenomenon of CNT is depressed (Fig. 3(b)). Subsequently, the alkylation of CNT–COOH

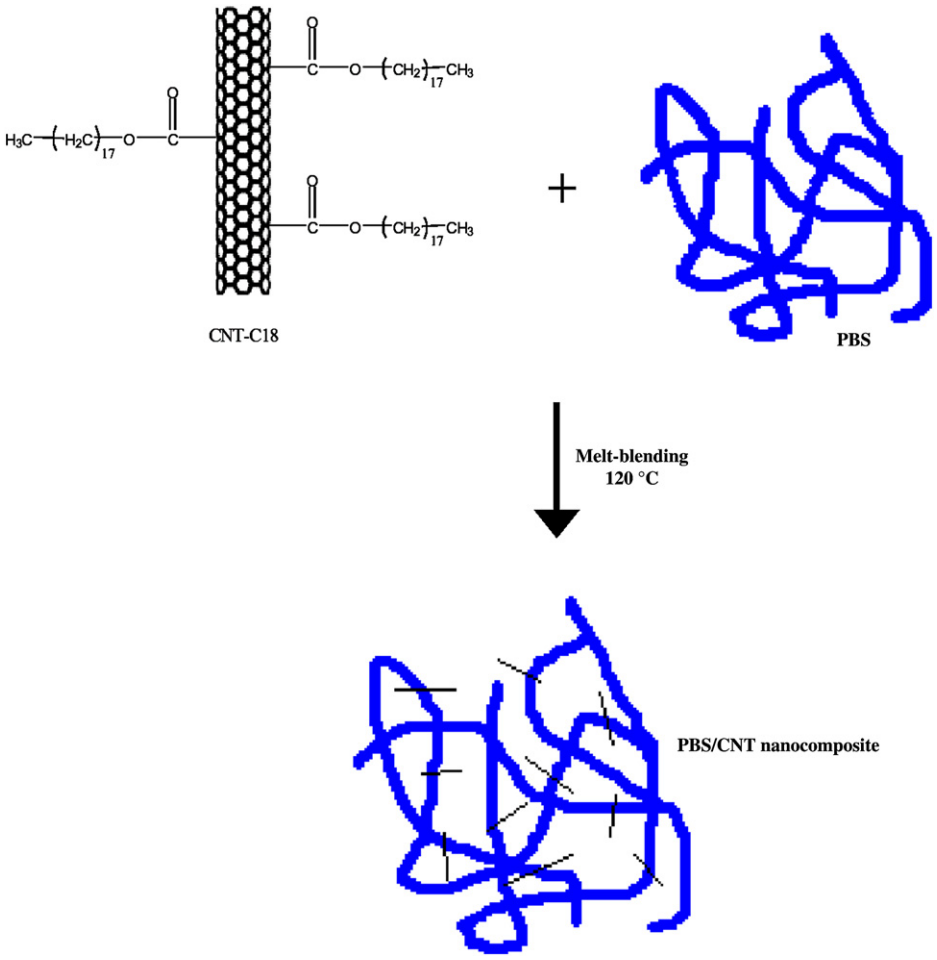

Scheme 3. Illustration of the melt-blending process.

to CNT–C18 would lead to the better solubility and dispersion of CNT in organic solvent (Fig. 3(c)).

3.2. Thermal properties of the PBS/CNT nanocomposites

Carbon nanotube is a material with excellent thermal stability. In the field of nanocomposites, carbon nanotubes can improve the thermal properties of nanocomposites. Table 1 shows the thermal decomposition temperatures (T_ds) of the nanocomposites, indicating that the addition of the CNTs increased T_d for the PBS/CNT nanocomposites. This is because the structure of nanotubes retards organic combustion and acts as a gas barrier that prevents the permeation of volatile gas out of the nanocomposites during thermal decomposition [26]. The T_d enhancement of the CNT–C18 system (from 367.2 to 379.5 °C) was more remarkable than that of the u-CNT system (from 367.2 to 374.0 °C). With the addition of

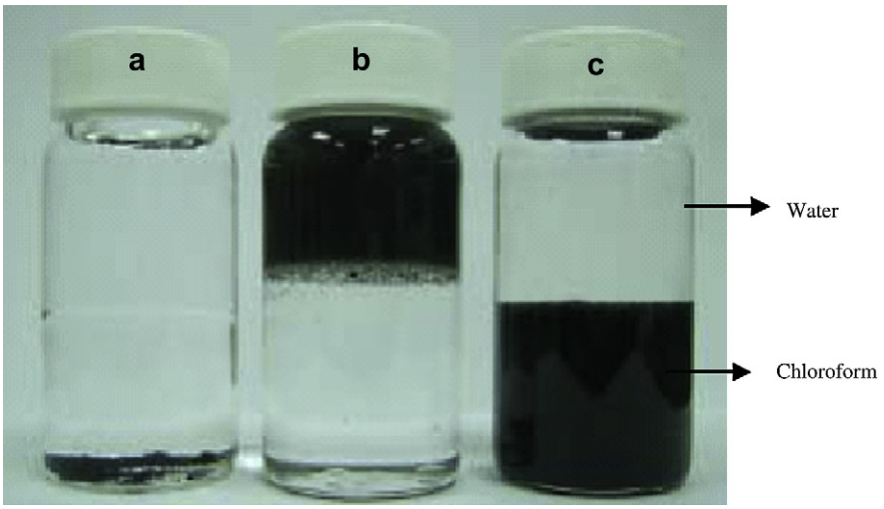

Fig. 1. Dispersion of (a) u-CNT; (b) CNT–COOH; (c) CNT–C18 in water/chloroform solution.

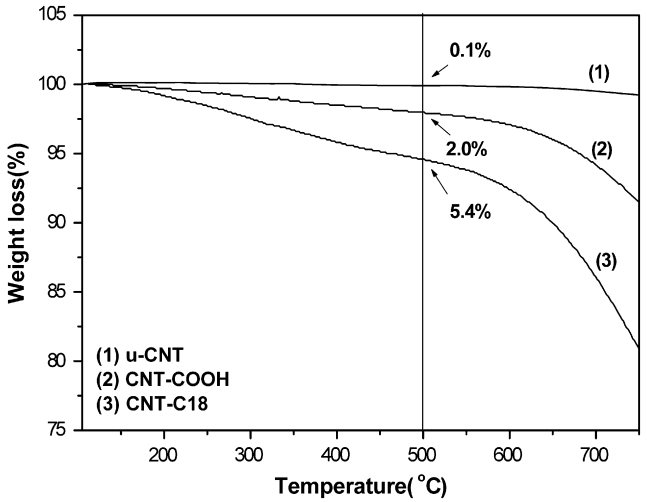

Fig. 2. TGA curves for (1) u-CNT; (2) CNT–COOH; (3) CNT–C18.

3 wt% CNT–C18, the T_d of the nanocomposite was increased as much as 12.3 °C. This suggests that CNT–C18 was dispersed homogenously in the PBS matrices along with a good interfacial adhesion [21].

Fig. 4 shows the DSC thermograms of the 1st cooling for PBS/u-CNT and PBS/CNT–C18 composites. The re-crystallization temperatures of the PBS/u-CNT and PBS/CNT–C18 composites were all higher than that of pristine PBS, and increased with increasing nanotube content, indicating that the CNTs played the role of nucleating agent and promoted the crystallization rate of PBS. It was also found that the re-crystallization peaks of PBS/CNT–C18 composites (Fig. 4(b)) were all sharper than those of PBS/u-CNT ones (Fig. 4(a)), indicating that the homogeneity of PBS/CNT–C18 composites is better than that of PBS/u-CNT ones, leading to a more obvious crystallization temperature. Similar phenomenon was also found in the DSC thermograms of the 2nd heating (Fig. 5). The melting peaks of PBS/CNT–C18 composites (Fig. 5(b)) were all sharper than those of PBS/u-CNT ones (Fig. 5(a)), indicating that the crystals in PBS/CNT–C18 composites were more regular than those in PBS/u-CNT ones. Moreover, two T_ms were found for both PBS/u-CNT and PBS/CNT–C18 systems in the thermograms. The temperature of the first T_m for the composites was much lower than that of pristine PBS. Most probably, they are connected with a minute fraction of thinner and/or less perfect crystals formed during the quenching of the films to room temperature after cold crystallization [27]. The temperature of the second T_m for the composites was similar to that of pristine PBS, and is more probable to refer to the melting point of the originally crystallized parts. The first T_m peak of the PBS/u-CNT composite was broader than that of the PBS/CNT–C18 ones. This indicates that thinner and/or less perfect crystals were formed in the u-CNT-containing matrices during the quenching process.

Table 1
T_ds of PBS/CNT nanocomposites

u-CNT or CNT–C18 (wt%)	PBS/u-CNT T_d (at 5 wt% weight loss) (°C)	PBS/CNT–C18 T_d (at 5 wt% weight loss) (°C)
0	367.2	367.2
1.5	368.6	373.9
3	374.0	379.5

3.3. Mechanical properties of the PBS/CNT nanocomposites

Fig. 6 shows variations of the storage modulus (E') with temperature for the PBS/CNT nanocomposites. E' was increased with increasing CNT–C18 content (Fig. 6(b)). This implies that CNT–C18 could enhance the rigidity of the nanocomposites. On the other hand, E' was increased with increasing u-CNT content at first, but then decreased with the addition of 3 wt% (Fig. 6(a)). This implies that the aggregation of u-CNT in the polymer matrices became pronounced as its content was larger than 1.5 wt%, and consequently led to poor mechanical performance. Moreover, the enhancements of the mechanical properties of the CNT–C18 system at various temperatures were more remarkable than those of the u-CNT system (Table 2). With the addition of 3 wt% u-CNT, the increment of E' of the nanocomposite at 25 °C was 84% (this value is very close to that of Ray et al.'s results measured at 28 °C, which was 88% [21]), whereas the increment of E' of the nanocomposite at 25 °C was up to 120% with the addition of 3 wt% CNT–C18 (Table 2). This indicates better dispersion of CNT–C18 than u-CNT in the PBS matrices.

Fig. 7 shows variations of the loss modulus (E'') with temperature for the PBS/CNT nanocomposites. E'' was increased with increasing CNT–C18 content (Fig. 7(b)). On the other hand, for the u-CNT-containing systems, the E'' of the 0.5 wt% u-CNT-containing sample was smaller than that of pristine PBS. E'' was then increased at 1.5 wt% content of u-CNT, but was decreased at 3 wt% content of u-CNT (Fig. 7(a)). The enhancements of the E'' properties of the

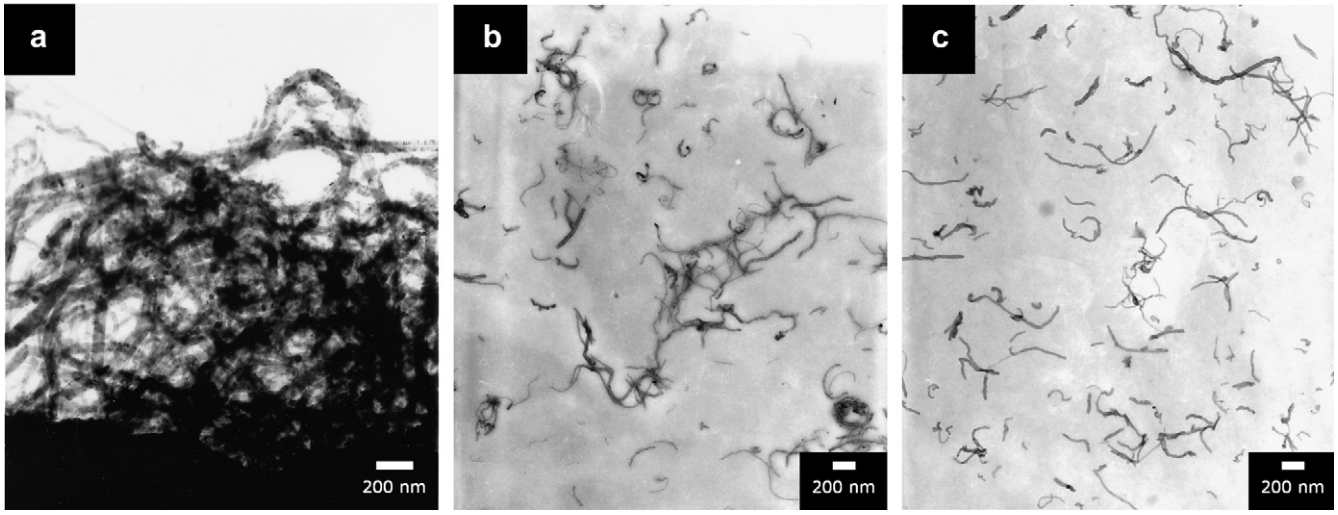

Fig. 3. Images of (a) u-CNT; (b) CNT–COOH; (c) CNT–C18.

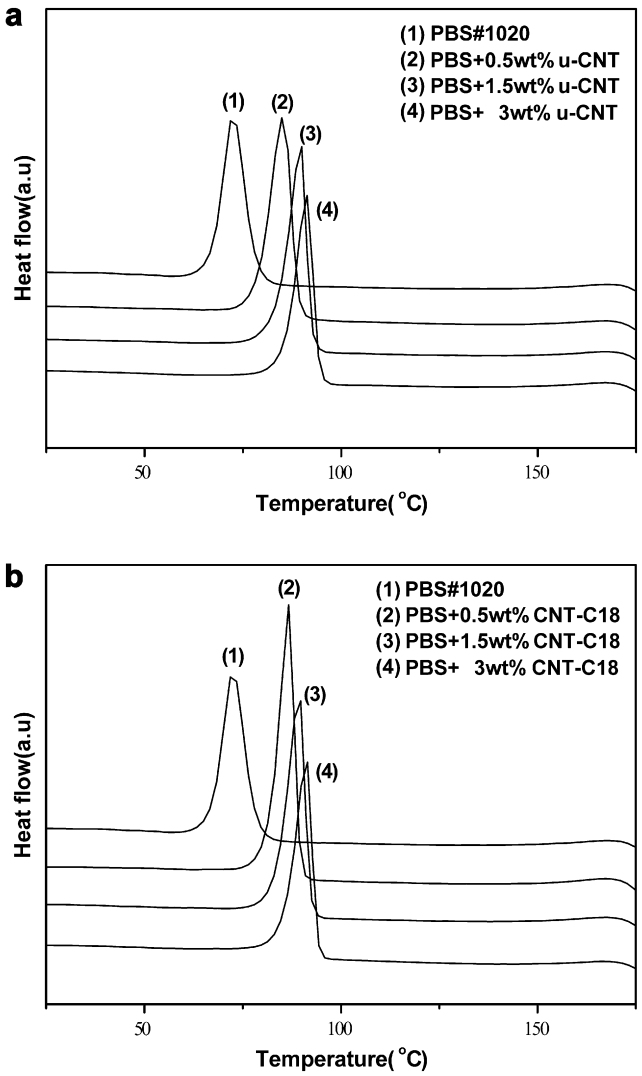

Fig. 4. DSC thermograms of (a) PBS/u-CNT; (b) PBS/CNT–C18 composites (1st cooling).

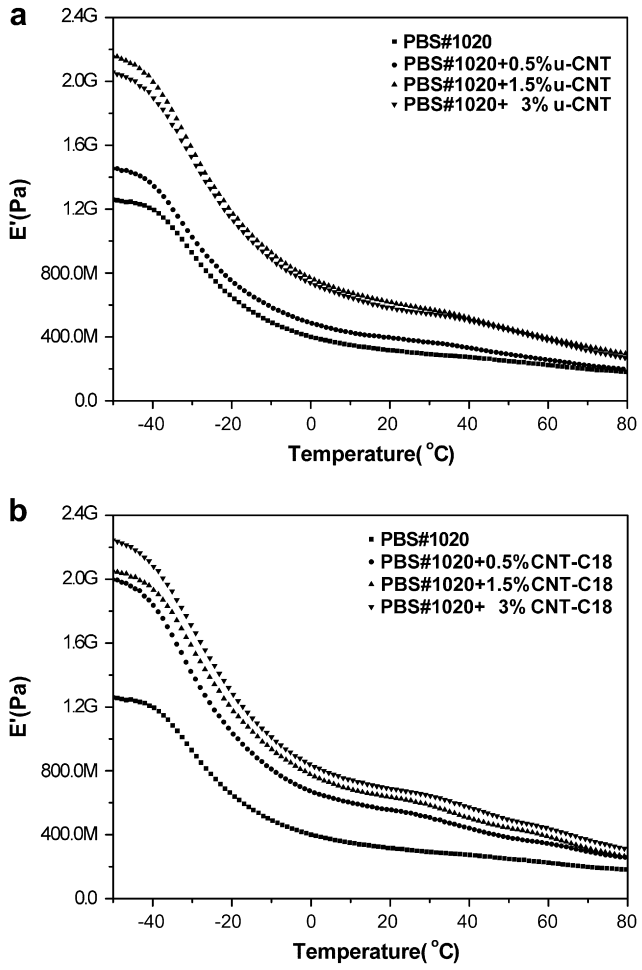

Fig. 6. Temperature dependence of storage moduli for (a) PBS/u-CNT; (b) PBS/CNT–C18 composites.

CNT–C18-containing systems were obviously more remarkable than those of the u-CNT-containing systems at 3 wt% doping levels at various temperatures (Table 3). With the addition of 3 wt% u-CNT, the increment of E'' of the nanocomposite at 25 °C was only 26%, but with the addition of 3 wt% CNT–C18, the increment of E'' of the nanocomposite at 25 °C was up to 55% (Table 3). From the results of the DMA measurement (Figs. 6 and 7), the enhanced mechanical properties could confirm that the modified carbon nanotubes (CNT–C18) were well dispersed in PBS matrices, and the interactions were greatly increased between PBS and CNT–C18.

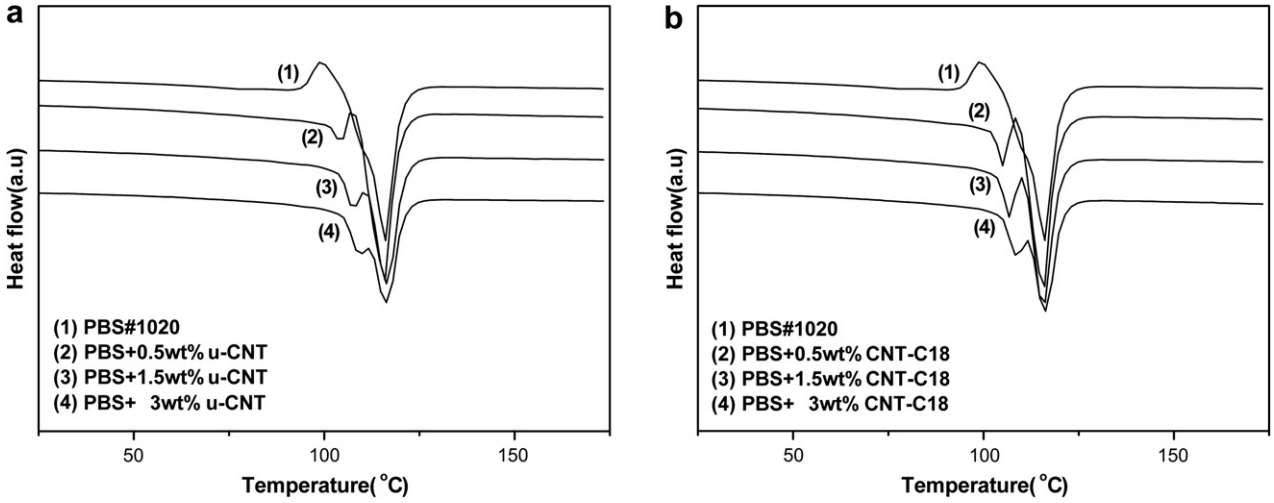

Fig. 5. DSC thermograms of (a) PBS/u-CNT; (b) PBS/CNT–C18 composites (2nd heating).

Table 2
Storage modulus of PBS/CNT nanocomposites

u-CNT or CNT–C18 (wt%)	E′ (Pa) and increment (%)[a] at −30 °C		E′ (Pa) and increment (%) at 0 °C	
	PBS/u-CNT	PBS/CNT–C18	PBS/u-CNT	PBS/CNT–C18
0	9.26×10^8	9.26×10^8	4.00×10^8	4.00×10^8
0.5	1.03×10^9 (11%)	1.41×10^9 (52%)	4.87×10^8 (22%)	6.72×10^8 (68%)
1.5	1.52×10^9 (64%)	1.57×10^9 (70%)	7.38×10^8 (85%)	7.75×10^8 (94%)
3	1.58×10^9 (71%)	1.70×10^6 (84%)	7.68×10^8 (92%)	8.37×10^8 (109%)
u-CNT or CNT–C18 (wt%)	E′ (Pa) and increment (%) at 25 °C		E′ (Pa) and increment (%) at 60 °C	
	PBS/u-CNT	PBS/CNT–C18	PBS/u-CNT	PBS/CNT–C18
0	3.04×10^8	3.04×10^8	2.25×10^8	2.25×10^8
0.5	3.81×10^8 (25%)	5.36×10^8 (76%)	2.56×10^8 (14%)	3.45×10^8 (53%)
1.5	5.95×10^8 (96%)	6.13×10^8(102%)	3.79×10^8 (68%)	3.88×10^8 (72%)
3	5.60×10^8 (84%)	6.68×10^8(120%)	3.94×10^8 (71%)	4.40×10^8 (96%)

[a] Increment (%) = 100% × (E′ (nanocomposite) − E′ (PBS))/E′ (PBS).

Table 3
Loss modulus of PBS/CNT nanocomposites

u-CNT or CNT–C18 (wt%)	E″ (Pa) and increment (%)[a] at −30 °C		E″ (Pa) and increment (%) at 0 °C	
	PBS/u-CNT	PBS/CNT–C18	PBS/u-CNT	PBS/CNT–C18
0	1.03×10^8	1.03×10^8	3.76×10^7	3.76×10^7
0.5	1.04×10^8 (1%)	1.42×10^8 (38%)	3.98×10^7 (6%)	5.14×10^7 (37%)
1.5	1.44×10^8 (40%)	1.36×10^8 (32%)	6.16×10^7 (76%)	5.80×10^7 (54%)
3	1.26×10^8 (22%)	1.45×10^8 (41%)	5.52×10^7 (47%)	6.49×10^7 (73%)
u-CNT or CNT–C18 (wt%)	E″ (Pa) and increment (%) at 25 °C		E″ (Pa) and increment (%) at 60 °C	
	PBS/u-CNT	PBS/CNT–C18	PBS/u-CNT	PBS/CNT–C18
0	1.96×10^7	1.96×10^7	1.63×10^7	1.63×10^7
0.5	1.82×10^7 (-7%)	2.25×10^7 (15%)	1.32×10^7(-19%)	1.57×10^7 (-4%)
1.5	2.84×10^7 (45%)	2.55×10^7 (30%)	2.27×10^7 (39%)	1.95×10^7 (20%)
3	2.47×10^7 (26%)	3.04×10^7 (55%)	1.91×10^7 (17%)	2.34×10^7 (44%)

[a] Increment (%) = 100% × (E″ (nanocomposite) − E″ (PBS))/E″ (PBS).

Glass transition temperatures (T_gs) measured from the peak temperature of E″ of the PBS/u-CNT (from −33.1 to −31.4 °C) and PBS/CNT–C18 (from −33.1 to −30.1 °C) nanocomposites were increased slightly [25] with increasing nanotube content (Table 4). This is because the nanotubes' structure would hinder segmental motions of the polymer chains [10], leading to the enhancement of T_g.

Table 4
T_gs (from E″ peak) of PBS/CNT nanocomposites

u-CNT or CNT–C18 (wt%)	PBS/u-CNT T_g (°C)	PBS/CNT–C18 T_g (°C)
0	−33.1	−33.1
0.5	−32.2	−32.0
1.5	−31.6	−30.3
3	−31.4	−30.1

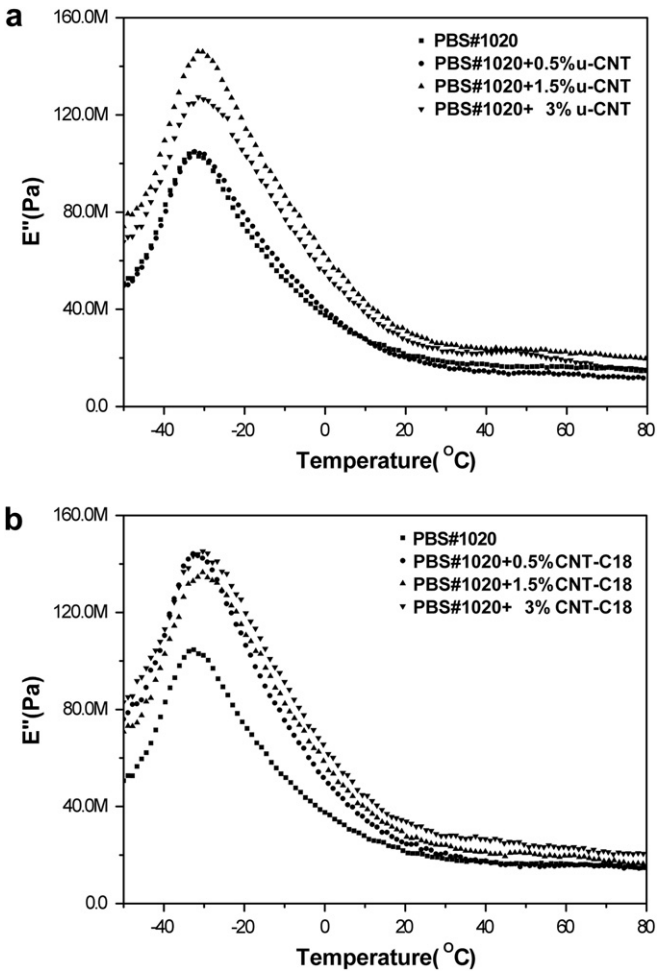

Fig. 7. Temperature dependence of loss moduli for (a) PBS/u-CNT; (b) PBS/CNT–C18 composites.

3.4. Electrical properties of the PBS/CNT nanocomposite

Table 5 shows the effect of u-CNT/CNT–C18 on the surface resistivity of PBS/CNT composites. At very low content of CNTs, the surface resistivity gradually decreased with increasing nanotube content. Multi-walled carbon nanotubes in the polymer matrices can connect with each other, and subsequently form an interconnecting conductive pathway, meaning an electrical percolation threshold. In other words, at the loading of MWNT, a very high percentage of electrons is permitted to flow through the sample with an applied electric field due to the creation of the interconnecting conductive channels [28–31]. The surface resistivity was decreased from "$>10^{16}$ Ω" (pristine PBS) to "1.39×10^9 Ω" with the addition of 3 wt% u-CNT, a decrease of about 10^7 fold in value of the electrical resistivity. This is very close to the results reported by Ray et al. [21]. According to their study, the in-plane conductivity increased from 5.8×10^{-9} S/cm for neat PBS to 4.4×10^{-3} S/cm for 3 wt% CNT-containing nanocomposite, an increase of 10^6 fold in the value of the electrical conductivity. On the other hand, the surface resistivity of the PBS/CNT–C18 composites decreased from "$>10^{16}$ Ω" (pristine PBS) to "7.30×10^6 Ω" for 3 wt% CNT–C18 composites, a decrease of over 10^9 fold in the value of the electrical resistivity. The decrease of surface resistivity of PBS/CNT–C18 composites was obviously larger than that of PBS/u-CNT composites, indicating the better dispersion of CNT–C18 in the polymer matrices as compared with that of u-CNT. This implies that the percolation thresholds of electrical conductivity were depressed. For this reason, the well-dispersed CNT–C18 in the PBS matrices

Table 5
Surface resistivity of PBS/CNT nanocomposites

u-CNT or CNT–C18 (wt%)	PBS/u-CNT surface resistivity (Ω)	PBS/CNT–C18 surface resistivity (Ω)
0	$>10^{16}$	$>10^{16}$
0.5	3.76×10^{14}	3.37×10^{13}
1.5	3.76×10^{11}	9.91×10^9
3	1.39×10^9	7.30×10^6

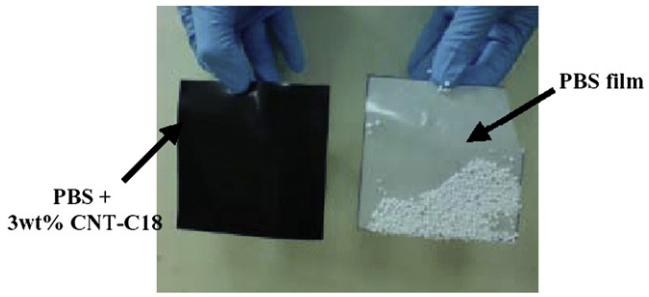

Fig. 8. Anti-static test.

could easily connect with each other. Therefore, the amount of CNTs needed to construct a conductive pathway was reduced [26]. Even though the resistivity values of the composite are not in the range of 'conductive materials', their resistivity is in the range of dissipative materials. In general, electric resistance between 10^8 and 10^{12} Ω would be capable of serving for anti-static function [32]. Fig. 8 compares the anti-static function of pristine PBS and 3 wt% CNT–C18-containing sample. These two films were firstly abraded, and then placed among foamed plastic balls. Evidently, the balls were adsorbed on the PBS film, but were not found on the CNT–C18-containing sample. This indicates that the PBS/CNT–C18 nanocomposite is able to serve the purpose of electrostatic discharge.

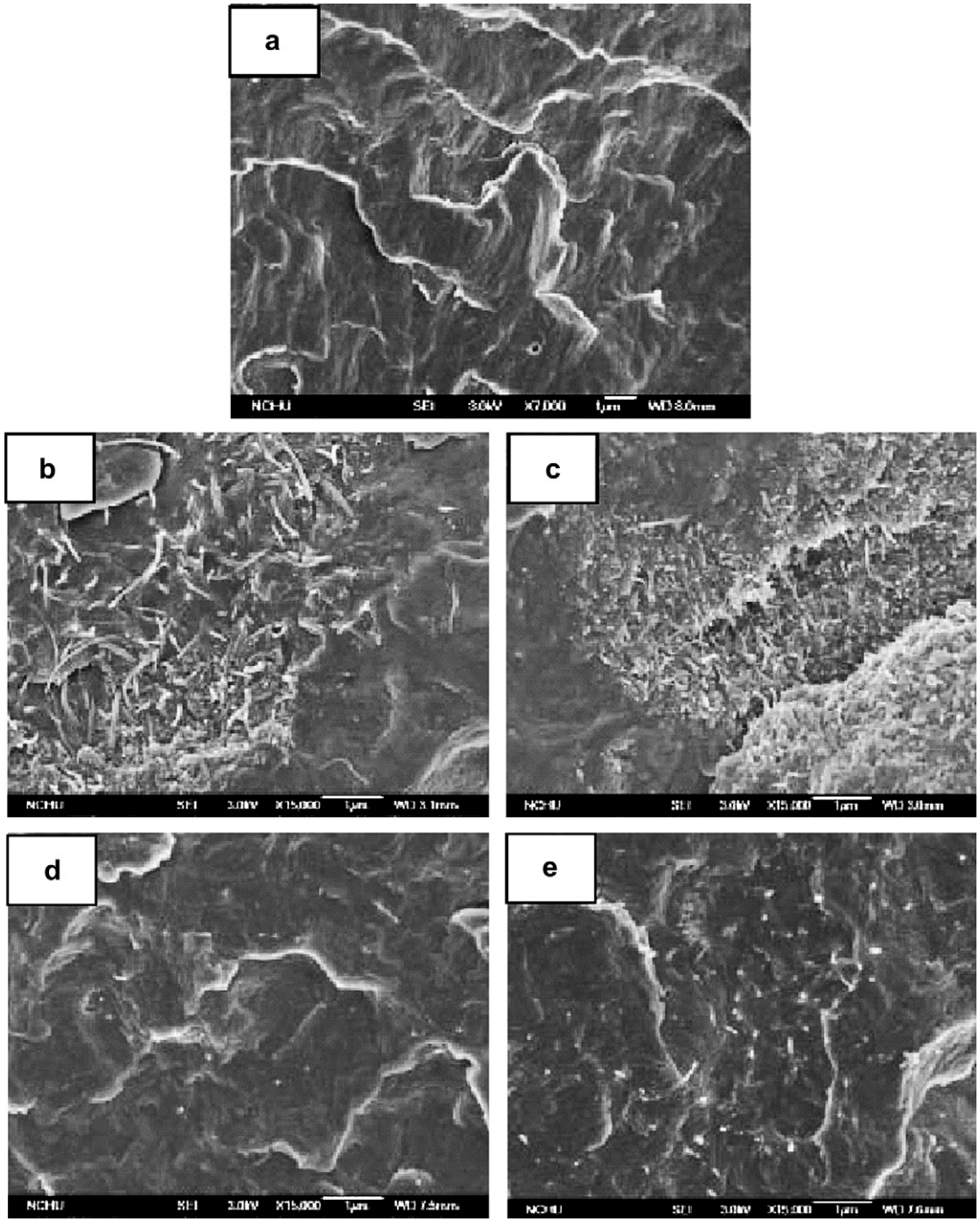

Fig. 9. SEM images of the fractured surface of PBS/CNT nanocomposites: (a) PBS; (b) 1.5 wt% u-CNT; (c) 3 wt% u-CNT; (d) 1.5 wt% CNT–C18; (e) 3 wt% CNT–C18.

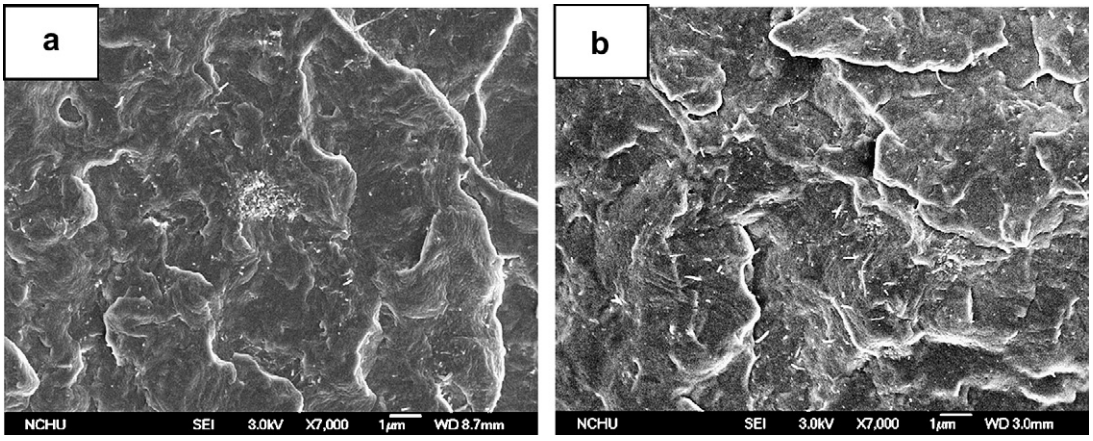

Fig. 10. SEM images of the fractured surface of PBS/CNT nanocomposites: (a) 3 wt% u-CNT; (b) 3 wt% CNT–C18 (×7k).

3.5. Morphology of PBS/CNT nanocomposites

The morphology and dispersion of the carbon nanotubes in polymer matrices were investigated using scanning electron microscopy (SEM) and transmission electron microscopy (TEM) [25]. As shown in the SEM photo of PBS/CNT nanocomposites (Fig. 9), many entangled clusters of u-CNT in PBS matrices were observed (Fig. 9(b) and (c)). Apparently, CNT–C18 dispersed homogenously in PBS matrices (Fig. 9(d) and (e)), which indicates that CNT–C18 is more compatible with the PBS matrices as compared with u-CNT. Better dispersion of CNT–C18 in PBS/CNT nanocomposites was due to the chemical modification of the u-CNT, which would bring about better compatibility with PBS [33].

SEM images of the fractured surfaces of 3 wt% u-CNT and 3 wt% CNT–C18 nanocomposites are shown in Fig. 10. The surface of 3 wt% CNTC18 nanocomposite was more wave-patterned as compared with that of 3 wt% u-CNT nanocomposite. This indicates that the toughness of PBS was enhanced more significantly by the addition of CNT–C18 than that of u-CNT [34].

TEM images of the PBS/CNT nanocomposites show the dispersion of the CNTs in the PBS matrices (Fig. 11). Fig. 11(a) and (b) shows the typical TEM images of u-CNT in the nanocomposites; the black spots correspond to aggregations of nanotubes. With increasing u-CNT content, the circumstances of aggregations and entanglements of u-CNT were more pronounced. Fig. 11(c) and (d) shows many individual tubes (CNT–C18) in the PBS matrices, along with more uniform dispersion of CNT–C18 with a small quantity of aggregates found.

Both results of SEM and TEM show that the nanotubes were more compatible with the PBS matrices after the chemical modification, leading to better thermal, mechanical and electrical properties.

4. Conclusion

We have successfully modified CNTs by using DCC dehydrating agents. The modified CNT–C18 sample could be well dispersed in organic solvents, and incorporated into the PBS matrices through

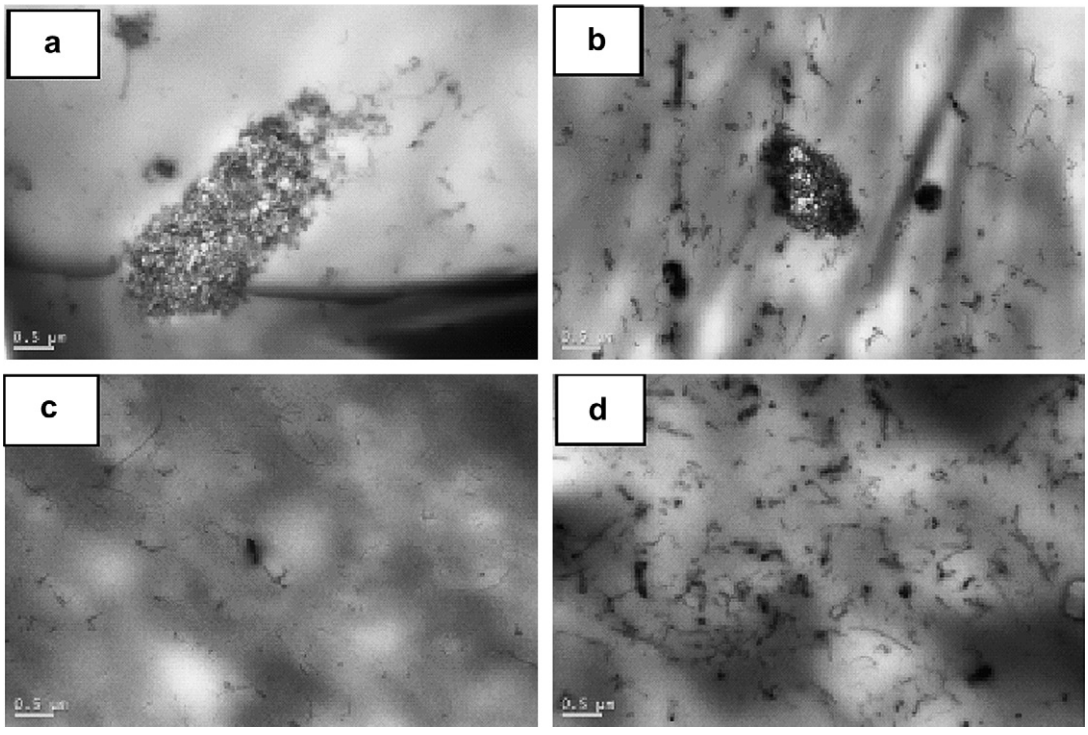

Fig. 11. TEM images of PBS/CNT nanocomposites: (a) 1.5 wt% u-CNT; (b) 3 wt% u-CNT; (c) 1.5 wt% CNT–C18; (d) 3 wt% CNT–C18.

simple melt blending. The results obtained show that the PBS/CNT–C18 nanocomposites exhibited not only a good dispersion of nanotubes in the PBS matrices, but also an improvement in thermal and mechanical properties as well. The decomposition temperature of the nanocomposite can be increased up to 12.3 °C, and the increment of E' and E'' of the nanocomposite at 25 °C can be achieved to 120 and 55%, respectively, as compared with the neat PBS sample. Moreover, a decrease of over 10^9 fold in value of the electrical resistivity and excellent anti-static capacity were found for the composite with 3 wt% CNT–C18.

Acknowledgements

Shih thanks National Science Council of Taiwan for financial support (NSC 95-2221-E-324-055). Jeng and Chen acknowledge partial financial support by Education Ministry of Taiwan, under the ATU plan.

References

[1] Shih YF, Chieh YC. Macromol Theory Simul 2007;16:101.
[2] Lim ST, Hyun YH, Choi HJ, Jhon MS. Chem Mater 2002;14:1839.
[3] Mani R, Bhattacharya M. Eur Polym J 2001;37:515.
[4] Ujimaki T. Polym Degrad Stab 1998;59:209.
[5] Iijima S. Nature 1991;354:56.
[6] Baughman RH, Zakhidov AA, de Heer WA. Science 2002;297:787.
[7] Thostenson ET, Ren ZF, Chou TW. Compos Sci Technol 2001;61:1899.
[8] Cheah K, Simon GP, Forsyth M. Polym Int 2001;50:27.
[9] Ginzburg VV, Gendelman OV, Manevitch LI. Phys Rev Lett 2001;86:5073.
[10] Wu CS, Liao HT. Polymer 2007;48:4449.
[11] Hong CY, You YZ, Pan CY. Chem Mater 2005;17:2247.
[12] Gao C. J Phys Chem B 2005;109:11925.
[13] Chen J, Hamon MA, Hui H, Chen Y, Rao AM, Eklund PC, et al. Science 1998;282:95.
[14] Chen C, Zhang Y. J Phys D Appl Phys 2006;39:172.
[15] Lin ST, Wei KL, Lee TM, Chiou KC, Lin JJ. Nanotechnology 2006;17:3197.
[16] Moon SI, Jin F, Lee CJ, Tsutsumi S, Hyon SH. Macromol Symp 2005;224:287.
[17] Song W, Zheng Z, Lu H, Wang X. Macromol Chem Phys 2008;209:315.
[18] Chen GX, Kim HS, Park BH, Yoon JS. Macromol Chem Phys 2007;208:389.
[19] Kim HS, Park BH, Yoon JS, Jin HJ. Polym Int 2007;56:1035.
[20] Zeng H, Gao C, Yan D. Adv Funct Mater 2006;16:812.
[21] Ray SS, Vaudreuil S, Maazouz A, Bousmina M. J Nanosci Nanotechnol 2006;6:2191.
[22] Hamon MA, Hui H, Bhowmik P, Itkis HME, Haddon RC. Appl Phys A 2002;74:333.
[23] Tasis D, Tagmatarchis N, Bianco A, Prato M. Chem Rev 2006;106:1105.
[24] Zhao C, Ji L, Liu H, Hu G, Zhang S, Yang M, et al. Solid State Chem 2004;177:4394.
[25] Bokobza L. Polymer 2007;48:4907.
[26] Tseng CH, Wang CC, Chen CY. Chem Mater 2007;19:308.
[27] Kulinski Z, Piorkowska E. Polymer 2005;46:10290.
[28] Bai JB, Allaoui A. Composites Part A 2003;34:689.
[29] Hu G, Zhao C, Zhang S, Yang M, Wang Z. Polymer 2006;47:480.
[30] Sandlera J, Shaffera MSP, Prasseb T, Bauhoferb W, Schultea K, Windlea AH. Polymer 1999;40:5967.
[31] Zhang Q, Rastogi S, Chen D, Lippits D, Lemstra PJ. Carbon 2006;44:778.
[32] Harry SK, John VM. Handbook of fillers for plastics. New York: Van Nostrand Reinhold Co.; 1987.
[33] Saeed K, Park SY. J Appl Polym Sci 2007;104:1957.
[34] Wang Y, Deng J, Wang K, Zhang Q, Fu Q. J Appl Polym Sci 2007;104:3695.